Interaction of S100A8/S100A9−Arachidonic Acid Complexes with the Scavenger Receptor CD36 May Facilitate Fatty Acid Uptake by Endothelial Cells[†]

Claus Kerkhoff,*[,‡] Clemens Sorg,[‡] Narendra N. Tandon,[§] and Wolfgang Nacken[‡]

Institute of Experimental Dermatology, D-48149 Münster, Germany, and Otsuka America Pharmaceutical Inc., Rockville, Maryland 20850

Received July 31, 2000; Revised Manuscript Received October 13, 2000

ABSTRACT: Recently, we showed that S100A8/A9 were secreted from phorbol ester-stimulated neutrophil-like HL-60 cells, thereby carrying arachidonic acid [Kerkhoff et al. (1999) *J. Biol. Chem. 274*, 32672−32679]. The present study was undertaken to evaluate whether the secreted S100A8/A9−AA complex might be involved in transcellular eicosanoid metabolism. In the presence of S100A8/A9, arachidonic acid was rapidly taken up by human umbilical vein endothelial cells in a saturable and energy-dependent fashion. Protein-facilitated arachidonate uptake was confirmed by its sensitivity toward the protein modifiers bromobimane and phloretin. Both potassium and sodium depletion did not affect the arachidonate transport, indicating that arachidonate influx was independent of endocytosis. The uptake of exogenous arachidonic acid by HUVEC was predominantly mediated by FAT/CD36. This conclusion was drawn by the findings that (i) arachidonate uptake was drastically inhibited by sulfo-*N*-succinimidyl oleate, a specific inhibitor of FAT/CD36; (ii) the maximal inhibition of arachidonate uptake induced by SSO was similar to that effected by ATP depletion; and (iii) the arachidonate transport was 2-fold higher in COS-7 cells transfected with the pEF.BOS-CD36 expression vector than in the empty vector-transfected COS-7 cells. Kinetic studies of arachidonate uptake were indicative for an interaction between fatty acid transporter and S100A8/A9−AA complex that was confirmed by an in vitro protein−protein interaction assay. FAT/CD36 has been suggested to be involved in inflammatory responses, and S100A8/A9 are released from activated leukocytes at inflammatory loci. Therefore, it can be envisioned that their interaction might propagate host response by perpetuating recruitment and activation of cellular effectors.

Adhesion of neutrophils to vascular endothelial cells is a characteristic feature of inflammation and involves numerous adhesion proteins that regulate their transmigration across the vascular endothelial barrier. The microenvironment at the interface between adherent neutrophils and endothelial cells represents a strategic site for exchange, transcellular synthesis, and metabolism of lipid mediators (for review, see *1*−*4*). Transcellular metabolism of eicosanoid intermediates produced by one cell type in close contact with another may amplify the formation of a given compound or result in products that neither of the participating cell types can generate alone (for review, see *5*, *6*). In addition, several reports indicate that endothelial cells and neutrophils utilize both endogenous and exogenous arachidonic acid for eicosanoid biosynthesis (*7*, *8*). Thus, liberation of arachidonate from cellular membranes as well as uptake of exogenous arachidonate increases the level of this otherwise rate-limiting substrate. At present, little is known about the membrane proteins involved in arachidonate uptake. The expression of one putative fatty acid transporter, the plasma membrane-bound fatty acid-binding protein ($FABP_{pm}$),[1] has been demonstrated on the surface of endothelial cells (*9*), and the participation of a yet unknown membrane protein in the free fatty acid (FFA) uptake by neutrophils was found by Krischer et al. (*10*).

Long-chain fatty acid (LCFA) uptake exhibits the kinetic features of a facilitated transport, including saturation, specificity, competitive inhibition (*11*−*13*), and sensitivity toward protein modifiers (*14*−*16*). Extensive investigations have determined that fatty acids are bound to albumin and other proteins in the extracellular space. However, the free fatty acid is the ligand for fatty acid transporters located at the plasma membrane. Five candidate proteins have been identified as putative FFA transporters: the plasma membrane-bound fatty acid-binding protein ($FABP_{pm}$) (*17*, *18*), the 56-kDa renal FABP (*19*), the 22-kDa plasma membrane protein caveolin (*13*), the fatty acid transport protein (FATP) (*20*), and the fatty acid translocase (FAT)/CD36 (*21*, *22*). These putative fatty acid transporters are expressed in a wide variety of tissues. For many cell types, it is not clear what the physiological significance of multiple transporters might imply (for review, see *23*).

[†] This work was supported by grants from the "Interdisziplinäres Zentrum für Klinische Forschung (IZKF)/Projekt C15" at the University of Münster.

* Address correspondence to this author at the Institute of Experimental Dermatology, Von-Esmarch-Strasse 56, D-48149 Münster, Germany. Phone: + 049-251-8356552. FAX: + 049-251-8356549. E-Mail: kerkhoc@uni-muenster.de.

[‡] Institute of Experimental Dermatology.

[§] Otsuka America Pharmaceutical Inc.

[1] Abbreviations: AA, arachidonic acid; FABP, fatty acid-binding protein; FA, fatty acids; $FABP_{pm}$, plasma membrane FABP; FAT, fatty acid transporter; FATP, fatty acid transport protein; FFA, free fatty acids; HUVEC, human umbilical vein endothelial cells; LCFA, long-chain fatty acids; SSO, sulfo-*N*-succinimidyl oleate.

10.1021/bi001791k CCC: $20.00
Published on Web 12/07/2000

Recently, we demonstrated that a protein complex formed by the two myeloid-related proteins MRP8 (S100A8) and MRP14 (S100A9) is secreted from phorbol ester-stimulated neutrophil-like HL-60 cells, thereby carrying arachidonic acid (AA) (*24*). The location of the effects induced by physiological stimuli, such as the chemoattractants FMLP and C5a (*25*), indicates that the secretion of S100A8/A9 takes place at inflammatory loci. The presence of S100A8/A9 complexes at sites of acute and chronic inflammation has long been noted (*26*−*28*), and there is definitive evidence that these proteins are specifically secreted into the extracellular space upon phagocyte activation (*29*). Both S100A8 and S100A9 belong to the S100 family of calcium-binding proteins (for review, see *30*, *31*). They are expressed in cells of the myeloid lineage and are predominantly localized in the cytoplasm (*32*, *33*). They specifically bind polyunsaturated fatty acids in a calcium-dependent manner (*34*, *35*) and represent the exclusive AA-binding capacity in the neutrophilic cytosol. To date, the exact functions of the proteins, especially in the extracellular milieu, remain unknown. We have speculated that S100A8/A9−AA complexes may serve as a transport protein to move AA to its target cells, representing a particular transcellular pathway for eicosanoid metabolism.

The present study was performed to characterize the fatty acid transporter on endothelial cells and to investigate whether AA was taken up by target cells in the presence of S100A8/A9. We present evidence that (1) the uptake of exogenous arachidonic acid by human umbilical vein endothelial cells (HUVEC) was predominantly mediated by FAT/CD36AA and (2) S100A8/A9 was bound to FAT/CD36, representing the first functional identification of a receptor for S100A8/A9.

EXPERIMENTAL PROCEDURES

Cell Culture. Human umbilical vein endothelial cells (HUVEC) were cultured in endothelial growth medium (EGM) supplemented with 12 μg/mL bovine brain extract, 10 ng/mL human epidermal growth factor, 1 μg/mL hydrocortisone, 0.1% GA-1000 (gentamicin, amphotericin-B), and 5% fetal bovine serum (Clonetics).

Measurement of Arachidonic Acid Uptake. S100A8 and S100A9 were purified from human neutrophils according to the method of Kerkhoff et al. (*24*). The arachidonate/fatty acid-binding protein complexes were formed as described earlier (*24*). HUVEC were plated at a density of 5×10^5 cells/well onto 24-mm tissue culture dishes for 24 h at 37 °C in EGM containing the above supplements. Prior to use, the cells were washed twice with serum-free medium and then incubated with either [^{3}H]AA−BSA or [^{3}H]AA−S100A8/A9 complexes at 4 and 37 °C for different time intervals as indicated. The [^{3}H]AA uptake was stopped by adding ice-cold 0.9% NaCl, 0.5% fatty acid-free BSA, and thereafter the cells were incubated for a further 5 min at 4 °C. The supernatant was then discarded, and the cells were washed again with the stop solution. Next, the cells were solubilized in 200 μL/well 0.2 M NaOH for 2 h at 37 °C. After the addition of 0.2 M HCl and 1.5 M Tris-HCl, pH 8.8 (200 μL each), the cell homogenate was transferred into scintillation vials, and cell-associated radioactivity was determined after the addition of 5 mL of scintillation cocktail using a LKB 1211 rackbeta counter.

Physiochemical Maneuvers of AA Uptake. For ATP depletion, the cells were incubated for 30 min at 37 °C prior to AA uptake measurements with ATP depletion buffer [140 mM NaCl, 20 mM HEPES (pH 7.4), 1 mM $CaCl_2$, and 1 mM $MgCl_2$] containing either 5 mM NaN_3 and 50 mM 2-deoxyglucose (ATP-depleted) or NaN_3 and 50 mM glucose (control). For potassium depletion, the cells were incubated for 30 min at 37 °C prior to AA uptake measurements with KCl depletion buffer [140 mM NaCl, 20 mM HEPES (pH 7.4), 1 mM $CaCl_2$, 1 mM $MgCl_2$, and 5.5 mM D-glucose] with 10 mM KCl (control) or without KCl (potassium-depleted). Carbonyl cyanide *m*-chlorophenylhydrazone (CCCP, 10 μM) and valinomycin (3 μM) were added to the cells 30 min at 37 °C prior to AA uptake measurements. Nigericin (3 μM), colchicine, democolcine, nocadazole, monesin, cytochalasin B, or cytochalasin D (each 10 μM) was added 60 min prior to AA uptake measurements. Sulfo-*N*-succinimidyl oleate (SSO) was prepared according to the method of Harmon et al. (*16*) with a few modifications. HUVEC were incubated with medium containing increasing concentrations of bromobimane (*p*-sulfobenzoyloxybromobimane, Calbiochem), phloretin (Sigma), or SSO for 30 min at 37 °C as indicated prior to measurements of arachidonate uptake.

^{125}I-Labeling of S100A8 and S100A9. Radioactive iodine was incorporated into the proteins as described by Markwell (*36*). Briefly, IODO-BEADS Iodination Reagent (Pierce) was added to 1 mCi of [^{125}I]NaI for 5 min at room temperature prior to the addition of 300 μg of S100A8/A9. The reaction was allowed to proceed for 15 min at room temperature and stopped by removing the solution from the beads. Finally, the radiolabeled protein was purified from excess [^{125}I]NaI or unincorporated [^{125}I]I_2 by gel filtration using PD10 desalting columns (Pharmacia).

RNA Preparation and Northern-Blot Analysis. Total RNA was prepared from liver or HUVEC by the acid guanidium thiocyanate−phenol−chloroform extraction method. Northern-blot analysis was performed according to standard protocols. The complementary synthetic oligonucleotides used for Northern-blot analysis were derived from published sequences: 5′-aacctataactggattcactttacaatttgcaaaacggctgcaggtcaac-3′ for FAT/CD36 [corresponding to nucleotide numbers 1331−1380 of the published human sequence (*37*, *38*) (GenBank accession number M24795)]; 5′-ctgtattccaacccacctctcaatggggcccggatcgcagcaaccatcct-3′ for mAspAT [corresponding to nucleotide numbers 971−1020 of the published mouse sequence (*39*) (GenBank accession number U82470)]; 5′-accgcactggggacacgttccgctggaaaggtgagaacgtgtccaccaccgaggtg-3′ for FATP [corresponding to nucleotide numbers 1504−1560 of the published human sequence (*40*) (GenBank accession number AF055899)]. After hybridization, membranes were washed and autoradiographed with an intensifying screen at −80 °C.

Transient Transfection of Plasmid cDNA into COS-7 Cells. The COS-7 cell line was routinely cultured in DMEM supplemented with 10% FCS. Transient transfection of plasmid DNA into COS-7 cells was performed using either the pEGFP-C1 or the pEF.BOS expression vector containing the human CD36 cDNA (*41*) insert as described by Melkonyan et al. (*42*) After electroporation, the cells were cultured for 48 h at 37 °C and 5% CO_2 before analysis of AA uptake.

Preparation of Platelets and Triton-X114 Solubilization. Isolation of human blood platelets and solubilization were performed according to Kronenberg et al. (*44*) with slight modifications. Briefly, platelets were solubilized for 30 min at 4 °C in 10 mM Tris-HCl (pH 7.4) containing 5 mM EDTA, 1% (v/v) Triton-X114. The suspension was centrifuged at 15000*g* for 1 h at 4 °C. The supernatant was carefully overlayered with 3 times its own volume of 6% sucrose in 154 mM NaCl, 1 mM EDTA, 0.06% (v/v) Triton-X114, 10 mM Tris-HCl (pH 7.4), rewarmed to 37 °C, and thereafter centrifuged at 1100*g* for 10 min at room temperature. The Triton-X114 phase was removed, and the upper phase was adjusted to 1% (v/v) Triton-X114 followed by sucrose gradient centrifugation as described above. The yellow Triton-X114 phases were collected and pooled.

Pull-Down Assay. Recombinant histidine-tagged proteins and glutathione-*S*-transferase (GST) fusion proteins were prepared as described earlier (*43*). Ten micrograms of GST−S100A8 fusion protein and 10 μg of his-tagged S100A9 were incubated in interaction buffer (TBS buffer supplemented with 20 mM imidazole and 1 mg/mL BSA) for 1 h at room temperature in a total volume of 500 μL. Then, either HUVEC membrane solubilizate or thrombocyte Triton phase was added, briefly vortexed, and incubated for a further 1 h at room temperature in a final volume of 1 mL. The 5% Ni−NTA magnetic agarose bead suspension (Qiagen) was washed in interaction buffer 3 times, and 50 μL of bed volume was added to the mixture. After 1 h incubation, the tubes were placed on a magnetic separator for 1 min, and the supernatants were discarded. The tubes were then removed from the magnet and the pellets washed twice with interaction buffer. Finally, SDS sample buffer was added to the pellets, the mixture was heated to 95 °C for 5 min, and the proteins were subjected to 12% SDS−PAGE (*45*). The Western-blot analysis was performed using standard protocols.

Protein Determination. Determination of protein content was performed according to Smith et al. (*46*), using BSA as standard. The concentrations of the purified proteins were accurately determined using the extinction coefficient of 0.998 for S100A8, 0.526 for S100A9, or 0.762 for S100A8/A9 at 280 nm, respectively.

RESULTS

Arachidonic Acid Uptake by HUVEC. To compare arachidonic acid (AA) uptake in the presence of either S100A8/A9 or bovine serum albumin, human umbilical vein endothelial cells (HUVEC, 10^5 cells/well) were incubated with 1 μM [^{3}H]AA and either 0.3 μM BSA or 2 μM S100A8/A9 at 4 or 37 °C for different time intervals as indicated. Based on the reported binding constant of AA for S100A8/A9 (*24*, *35*) and the BSA−AA constants published by Kleinfeld and colleagues (*47*), we calculated free fatty acid (FFA) concentrations at these fatty acid:fatty acid-binding protein ratios of 135 nM for BSA and 150 nM for S100A8/A9. Subsequently, cell-associated radioactivity was determined as described under Experimental Procedures.

As shown in Figure 1, the AA transport was significantly lower at 4 °C in the presence of both fatty acid-binding proteins. At 37 °C, the uptake of [^{3}H]AA was faster and revealed linearity during the incubation time, indicating that

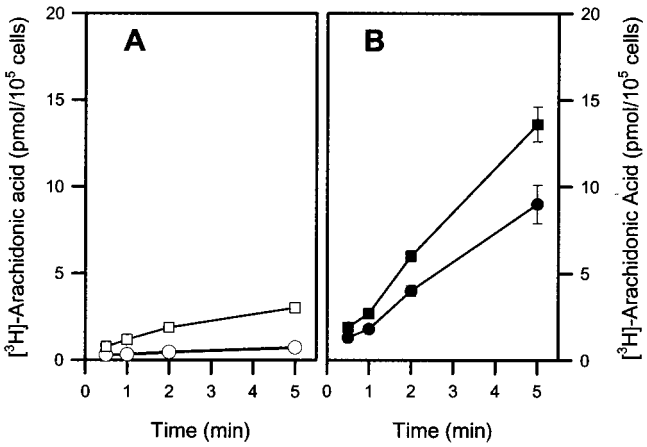

FIGURE 1: Time course of arachidonate uptake in HUVEC in the presence of either BSA or S100A8/A9. AA uptake was assayed by adding 1 μM [^{3}H]AA in the presence of either 0.33 μM BSA (●,○) or 2 μM S100A8/A9 (■,□) to HUVEC (10^5 cells/well) at 4 °C (A) or 37 °C (B). Details of the experiment are described under Experimental Procedures. Shown are means of triplicate determinations ± SD. (●) [^{3}H]AA−BSA, 37 °C; (○) [^{3}H]AA−BSA, 4 °C; (■) [^{3}H]AA−S100A8/A9, 37 °C; (□) [^{3}H]AA−S100A8/A9, 4 °C.

the FA uptake represents an energy-dependent transport process. Furthermore, the arachidonate uptake was significantly higher in the presence of S100A8/A9 than in the presence of BSA.

Next, we performed arachidonate uptake experiments in the presence of different fatty acid:fatty acid-binding protein ratios to estimate the kinetic constants of AA transport into HUVEC in the presence of either S100A8/A9 or BSA (Figure 2). When plotted as a function of free arachidonate concentrations, calculated by using the corresponding association constants (*24*, *47*), the rates of arachidonate uptake displayed saturation kinetics with a Michaelis−Menten relationship. Analysis of the data yielded V_{max} and K_M estimates of 14.1 ± 4.1 pmol min^{-1} (10^5 cells)$^{-1}$ and 173 ± 88 nM for S100A8/A9, 13.6 ± 2.1 pmol min^{-1} (10^5 cells)$^{-1}$ and 2.2 ± 0.7 nM for BSA, respectively. The calculated V_{max} values were in a similar range, although the K_M for arachidonate was significantly higher in the presence of S100A8/A9 than in the presence of BSA, indicative of competitive inhibition.

We then investigated whether the fatty acid was taken up in conjunction with S100A8/A9. Analogous uptake experiments using radioiodinated S100A8/A9 were performed as described above for the arachidonate uptake. However, there was neither a time- nor a temperature-dependent increase in cell-associated radioactivity (data not shown). Therefore, we conclude that the fatty acid was transported via the fatty acid transporter with S100A8/A9 remaining at the cell surface.

Cellular AA Uptake Exhibits Kinetic Features of Facilitated Transport. To characterize the molecular mechanism by which AA is taken up by HUVEC, two approaches were used: (i) cells were treated with inhibitors of oxidative phosphorylation, ionophores, or cytoskeleton-disrupting agents prior to AA uptake measurements; (ii) the participation of membrane receptors in AA transport was investigated using cell-impermeable protein modifiers.

Lowering the temperature to 0 °C diminished the initial arachidonate uptake to 10% of the control value (Figure 3A). Both ATP depletion of cells by sodium azide and uncoupling

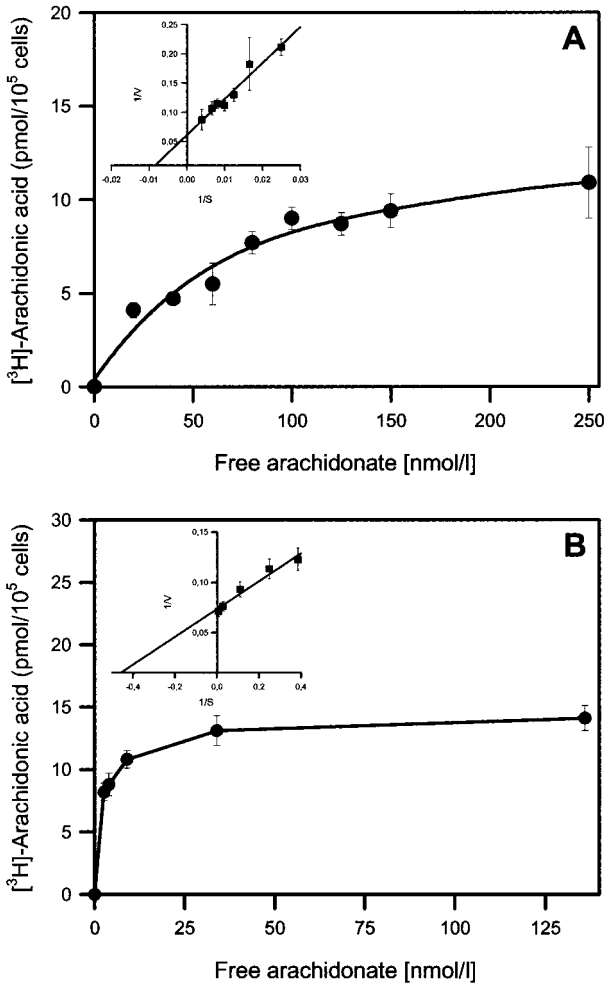

FIGURE 2: Kinetics of [^{3}H]AA uptake. Initial uptake of [^{3}H]AA was assayed at 37 °C for 120 s with free arachidonate concentrations from 20 to 250 nM in the presence of S100A8/A9 (A) or from 2.6 to 136 nM in the presence of BSA, respectively (B). Free fatty acid concentrations were determined using the published S100A8/A9−AA and BSA−AA binding constants (*7*, *47*). Insets: Corresponding Lineweaver−Burk plot of the same data. Linear regression yielded V_{max} and K_M estimates of 14.1 ± 4.1 pmol min^{-1} (10^5 cells)$^{-1}$ and 173 ± 88 nM for S100A8/A9 ($r^2 = 0.95$), 13.6 ± 2.1 pmol min^{-1} (10^5 cells)$^{-1}$ and 2.2 ± 0.7 nM for BSA ($r^2 = 0.97$), respectively. Values are means ± SD of $n = 4$ experiments.

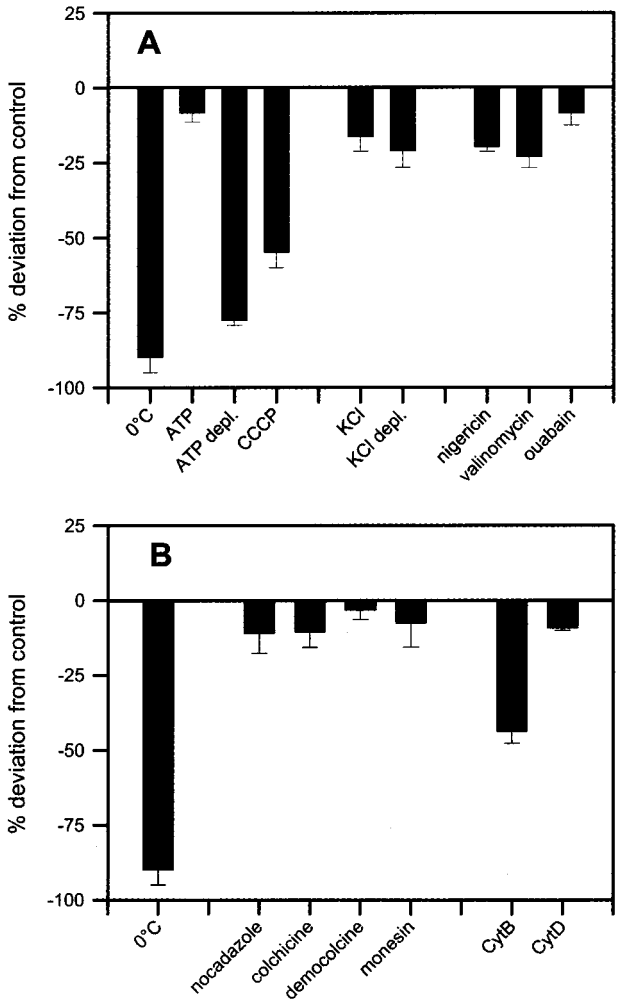

FIGURE 3: Influence of temperature reduction, ATP, sodium and potassium depletion (A), and depolymerization of the cytoskeleton (B) on initial arachidonic acid uptake rates. Uptake of [^{3}H]AA was assayed for 5 min with 1 μM AA/S100A8/A9 in the presence of the different agents as indicated. The details of the experiment are described under Experimental Procedures.

oxidative phosphorylation by 10 μM CCCP significantly lowered arachidonate uptake to 22.4 ± 1.7% and 45.0 ± 5.0% that of nondepleted cells, respectively (Figure 3A). These data clearly show that movement of arachidonate across the membrane represents an energy-dependent process.

The depletion of potassium as well as the preincubation of the cells with nigericin or valinomycin, both potent potassium ionophores, did not have a significant effect on the initial arachidonic acid uptake (Figure 3A). Preincubation of HUVEC with increasing concentrations of ouabain did not result in significant differences between the control and the depleted cells (data not shown). These data indicate that arachidonic acid uptake is independent of the formation of coated pits and endocytotic vesicles.

To verify this conclusion, analogous AA uptake studies were performed in the presence of cytoskeleton-disrupting agents since there is an intimate functional connection between the cytoskeleton and both receptor-mediated and fluid phase endocytosis (*48*, *49*). Only small effects were seen with colchicine, democolcine, and nocadazole (Figure 3B). These agents display antimicrotubular activity. Cytochalasin B has been shown to perturb the actin filament and suppressed the AA uptake by 40%. In addition to its cytoskeletal effects, cytochalasin B is an effective inhibitor of glucose uptake. Therefore, we also used cytochalasin D that is similarly effective as a cytoskeleton-disrupting agent but has no effect on glucose transport (*50*). Treatment with cytochalasin D did not affect the AA uptake by HUVEC. Thus, this study clearly indicates that the cytoskeleton is not involved in the uptake of AA bound to S100A8/A9.

To learn whether AA transport was facilitated by plasma membrane proteins, we incubated HUVEC with the protein modifiers bromobimane and phloretin prior to the uptake measurements (Figure 4). Bromobimane is not able to penetrate cells and reacts with thiol groups of membrane-bound proteins (*51*), thereby inhibiting receptor-mediated transport processes. Phloretin is described as potent nonspecific inhibitor of membrane transport proteins (*52*).

The inhibition of AA uptake was concentration-dependent for both agents, and an inhibition of 50% was reached at 10 μM bromobimane and 100 μM phloretin (Figure 4). The uptake kinetics and the inhibition of the arachidonate influx

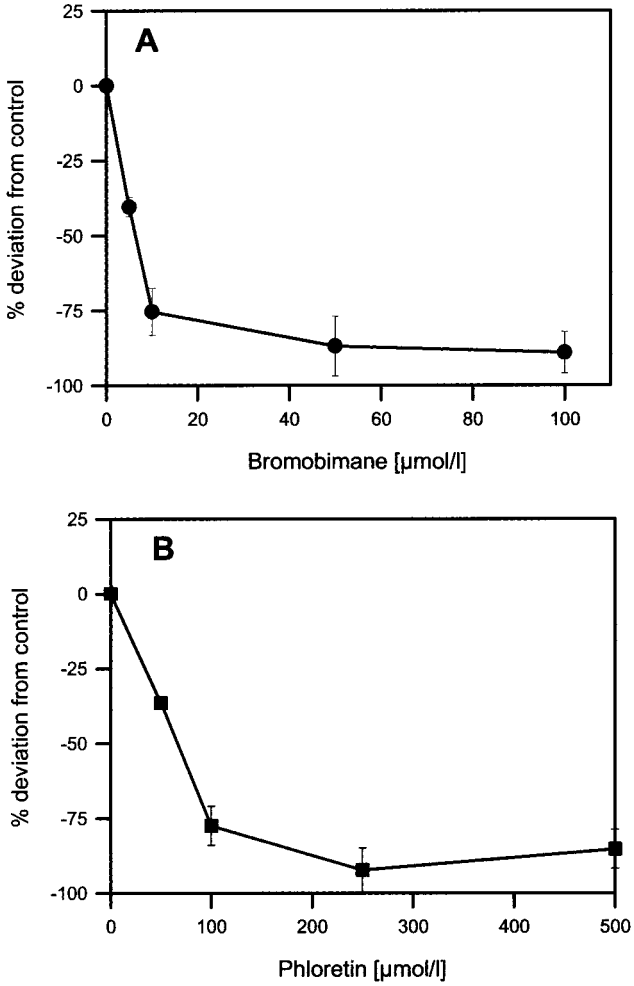

FIGURE 4: Inhibition of initial AA uptake by increasing concentrations of phloretin (A) and bromobimane (B) as indicated. HUVEC (10^5 cells/well) were preincubated with the agents as described under Experimental Procedures, and the uptake of [^{3}H]AA was assayed at 37 °C for 5 min. Values are means ± SD expressed as percent deviation from control. $n = 3$ experiments.

by bromobimane and phloretin strongly indicate that the uptake of AA in HUVEC was facilitated by a membrane receptor-regulated pathway. In control experiments, these agents had no effect on the fatty acid-binding capacity of the S100A8/A9 protein complex (data not shown).

Inhibition of Arachidonic Acid Uptake by Sulfo-N-succinimidyl Oleate. The fatty acid analogue sulfo-*N*-succinimidyl oleate (SSO) has been described as a specific, nontoxic, membrane-impermeable inhibitor of FAT/CD36 when preincubated with adipocytes for 25 min (*16*). When a similar procedure was applied here, AA uptake by HUVEC was drastically inhibited by SSO in a concentration-dependent manner (Figure 5). The half-maximal effect was seen at a concentration below 0.5 mM SSO with the maximal inhibition of AA uptake being ~80−90%, similar to that effected by ATP depletion. Together with the observed maximal inhibition by ATP depletion and temperature reduction (Figure 3A), we assume that FAT/CD36 represents the major fatty acid transporter on HUVEC although these results do not exclude the participation of other transport proteins.

AA Uptake in CD36-Transfected COS-7 Cells. To test whether FAT/CD36 promotes AA transport, the pEF.BOS expression vector containing a CD36 cDNA insert was

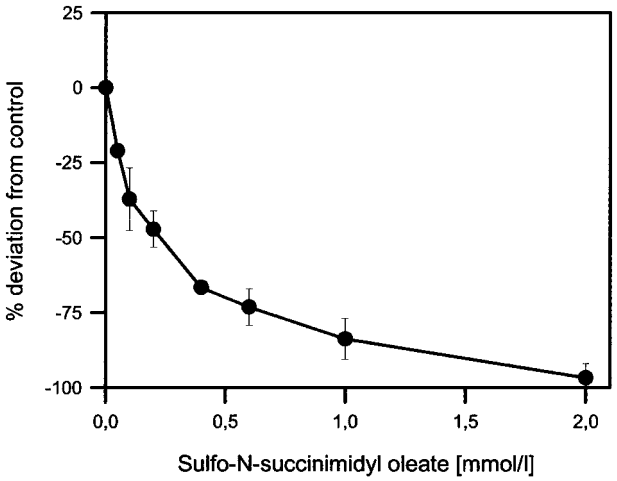

FIGURE 5: Inhibition of initial AA uptake by increasing concentrations of SSO as indicated. HUVEC (10^5 cells/well) were preincubated with SSO as described under Experimental Procedures, and the uptake of [^{3}H]AA was assayed at 37 °C for 5 min. Values are means ± SD expressed as percent deviation from control. $n = 3$ experiments.

transiently transfected into COS-7 cells (*41*). Plasmid DNA from the vector alone was transfected into COS-7 cells as a control. Cells were harvested 48 h after transfection, and cell lysates were analyzed for CD36 expression by Western-blot analysis. CD36 protein expression in vector-transfected COS-7 cells was very low, whereas the cells transfected with pEF.BOS-CD36 vector expressed higher levels of CD36 (data not shown). Immunohistochemical analysis of pEF-.BOS-CD36 vector-transfected cells revealed that CD36 protein was expressed on the cell surface and that 20−30% of the cells were positive for CD36 (data not shown).

We then performed analogous AA uptake experiments as described above for HUVEC using control and CD36-expressing COS-7 cells. The cells were incubated with 1 μM [^{3}H]AA−S100A8/A9 (molar ratio of fatty acid to fatty acid-binding protein 1:1) at 4 and 37 °C for different time intervals as indicated. The cell-associated radioactivity was determined as described under Experimental Procedures.

As shown in Figure 6A, CD36 expression resulted in a 2-fold increase in the initial arachidonic acid uptake at all time points measured when compared to vector-transfected COS-7 cells. The arachidonate uptake mediated by CD36 expressed by COS-7 cells was temperature-dependent, since the uptake at 4 °C was only 10% of that at 37 °C (data not shown). This suggested that a specific carrier-mediated process was involved in FA transport systems in COS-7 cells, and that the saturable component of fatty acid uptake could be modulated by CD36 expression. Kinetic studies of [^{3}H]-AA uptake revealed Michaelis−Menten constants of 666.7 ± 133.3 nM for CD36-negative and 1250 ± 250 nM for CD36-positive cells with maximum velocities of 8.6 ± 1.9 pmol min^{-1} (10^5 cells)$^{-1}$ for CD36-negative and 18.0 ± 3.7 pmol min^{-1} (10^5 cells)$^{-1}$ for CD36-positive cells, respectively (Figure 6B). These values were significantly different from each other.

Protein−Protein Interaction Assay with CD36 and S100A8/A9. We then used the in vitro pull-down assay to establish whether S100A8/A9 directly interacts with CD36 (Figure 7). CD36 partially purified from either thrombocytes or HUVEC was incubated with either the fusion protein GST−

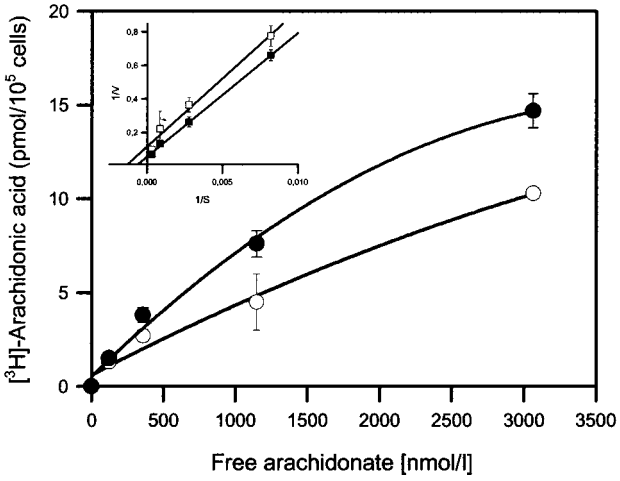

FIGURE 6: Time course of arachidonate uptake by CD36-expressing COS-7 cells 2 days posttransfection. The AA uptake was assayed by adding 1 μM [^{3}H]AA and 1 μM S100A8/A9 at 37 °C. Shown are means of representative experiments ± SEM. (●) CD36-positive cells; (○) CD36-negative cells. Inset: Lineweaver−Burk plot of the kinetics of [^{3}H]AA uptake in CD36-transfected cells. Linear regression revealed Michaelis−Menten constants of 666.7 ± 133.3 nM for CD36-negative and 1250 ± 250 nM for CD36-positive cells with maximum velocities of 8.6 ± 1.9 pmol min^{-1} (10^5 cells)$^{-1}$ for CD36-negative and 18.0 ± 3.7 pmol min^{-1} (10^5 cells)$^{-1}$ for CD36-positive cells, respectively. Shown are means of representative experiments ± SEM. (■) CD36-positive cells; (□) CD36-negative cells.

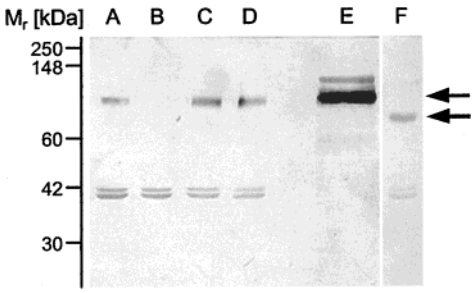

FIGURE 7: Protein−protein interaction assay. Prior to addition of magnetic beads, GST−S100A8, His$_6$-tagged S100A9, or partially purified CD36 from different fractions was incubated for 1 h at room temperature as indicated. The magnetic beads were washed followed by addition of SDS sample buffer. Then the suspension was heated to 95 °C, and the proteins were subjected to 12% SDS−PAGE followed by Western-blot analysis. (A) His$_6$-tagged S100A9 + Triton phase; (B) Triton phase; (C) His$_6$-tagged S100A9 + GST−S100A8 + Triton phase; (D) His$_6$-tagged S100A9 + GST−S100A8 + Triton phase + 1 mM $CaCl_2$; (E) thrombocytes; (F) His$_6$-tagged S100A9 + GST−S100A8 + HUVEC membrane solubilizate.

S100A8, histidine-tagged S100A9, or a combination of both recombinant proteins. Ni−NTA magnetic agarose beads were then added and washed twice with interaction buffer, and the proteins were eluted by the addition of SDS sample buffer. The proteins were subjected to 12% SDS−PAGE followed by Western-blot analysis.

Possible nonspecific binding of the CD36 protein to the affinity matrix was excluded by the finding that CD36 did not bind to the affinity matrix either in the absence of recombinant proteins or in the presence of GST alone. CD36 protein did bind to the Ni−NTA magnetic agarose beads by interaction with GST−S100A8/hisS100A9 or hisS100A9. Further analysis revealed that S100A8/A9 interacted with an 88-kDa protein partially purified from thrombocytes and with a 78-kDa protein from HUVEC membranes.

DISCUSSION

In the present study, we provide evidence that the uptake of exogenous arachidonic acid by HUVEC is predominantly mediated by FAT/CD36. Furthermore, this report describes the first functional characterization and identification of a cell surface protein that functions as a receptor for S100A8/A9. Our conclusions are based upon pharmacological (inhibition of CD36/FAT by its specific inhibitor SSO), protein (protein−protein interaction assay), and functional analyses (arachidonate uptake by HUVEC as well as CD36-transfected COS-7 cells).

The AA uptake by HUVEC exhibited many characteristic properties of a protein-mediated transport process: (i) The fatty acid uptake was shown to be temperature-dependent since the uptake at 4 °C was only 10% of that at 37 °C (Figure 3A). (ii) The kinetic studies revealed evidence that the FA uptake was dependent on an equilibrium between the free fatty acid concentration and the fatty acid-binding proteins (Figure 2). (iii) The AA uptake was inhibited by protein modifiers, indicating that membrane proteins are involved in arachidonate transport (Figure 4). (iv) The depletion of intracellular ATP as well as the exposure of the cells to metabolic inhibitors, such as CCCP, significantly lowered arachidonate uptake to 35% and 45% of that for nondepleted cells, respectively, indicating that the uptake is energy-dependent (Figure 3A). (v) Potassium plays an important role in the formation of coated pits and endocytotic vesicles. However, neither the depletion of potassium nor the preincubation of the cells with nigericin or valinomycin, both potent potassium ionophores, effected the movement of AA across the cell membrane (Figure 3A). In addition to the results from our studies using agents displaying cytoskeleton-disrupting activity (Figure 3B), our conclusion that fatty acids are taken up independently of endocytosis is in agreement with a hypothetical model for FA transport proposed by Abumrad and colleagues (*23*). They presented a model in which CD36, one of the fatty acid transporter candidates, facilitates AA transport by the formation of a multimeric pore or channel. In addition, Thorne et al. (*41*) reported that FAT/CD36 forms covalently associated dimers and multimers.

On the other hand, the uptake of arachidonate in the presence of S100A8/A9 complexes had some properties that differed from the reported mechanism of fatty acid transport. It was demonstrated by Abumrad and colleagues that free fatty acid but not the BSA-bound form is the ligand for CD36. However, our kinetic studies revealed evidence for an interaction between FAT/CD36 and S100A8/A9 because although the calculated V_{max} values were in the similar range the K_M values were quite different, indicative of competitive inhibition (Figure 2). In addition, the fatty acid transport was significantly higher in the presence of S100A8/A9 than in the presence of BSA. The protein−protein interaction assay revealed evidence that S100A8/A9 directly interacts with CD36 (Figure 7). Therefore, we suggest that the interaction of the S100A8/A9−AA complex with CD36 may accelerate the dissociation of the complex, which in turn would facilitate the uptake of fatty acids by the cells. The uptake experiments using radiolabeled S100A8/A9 exclude the possibility that S100A8/A9 itself is taken up by the cells. Thus, the fatty acid must be transferred from the complex to CD36 prior to

its transport. However, we cannot for certain exclude the alternative that S100A8/A9−AA forms an equilibrium and that the free AA is then transported.

The participation of CD36/FAT in AA transport by HUVEC is well documented by the following findings: (i) The AA uptake was drastically inhibited by the fatty acid analogue SSO (Figure 5). Several groups have confirmed that SSO is a specific inhibitor of CD36. It binds covalently to FAT/CD36 (*16*, *21*, *53*), and SSO inhibits LCFA transport in tissues that express FAT/CD36 (muscle and heart) but not in tissues in which FAT/CD36 is not expressed (i.e., liver) (*54*). However, when performing analogous [^{14}C]deoxyglucose uptake studies, SSO showed little inhibitory effect upon deoxyglucose uptake (data not shown). No decrease of 50% in deoxyglucose uptake was found in the range of 0−2 mM SSO. Maximal inhibition of deoxyglucose uptake was ∼30−40% at a 2 mM concentration of SSO. Due to our findings, that the maximal inhibition of AA uptake by SSO was ∼80−90% and the half-maximal effect was seen at a concentration below 0.5 mM SSO, we conclude that SSO is more effective in the inhibition of fatty acid uptake than in the inhibition of deoxyglucose uptake. The maximal inhibition of AA uptake by SSO was similar to that effected by ATP depletion (Figure 3A). (ii) Five plasma membrane proteins have been reported and proposed to function in fatty acid movement across the plasma membrane (for review, see *23*). Of the candidate transporters, three have been sequenced and cloned. Northern-blot analysis revealed the expression of $FABP_{pm}$, FATP, and FAT/CD36 in HUVEC (data not shown). The size of the mRNA transcripts was identical to those previously reported in other tissues (*20*, *22*, *55*). (iii) The expression of one putative fatty acid transporter, $FABP_{pm}$, was demonstrated at the surface of endothelial cells (*9*). It has been shown that the $FABP_{pm}$-facilitated oleate uptake by hepatocytes was sodium-dependent. The uptake was diminished when Li^+, K^+, choline, or sucrose was substituted for Na^+ in the incubation medium, and was reduced by 46% by ouabain, an inhibitor of Na^+−K^+-ATPase (*17*). In addition, the Na^+-dependent FA uptake was found to be stimulated by valinomycin (*56*). However, in our studies the preincubation with ouabain was without significant effect on initial arachidonic acid uptake (Figure 3A). Therefore, these data give additional evidence that $FABP_{pm}$ did not represent the membrane protein facilitating AA uptake by HUVEC. (iv) Strong evidence for CD36 as a fatty acid transporter was established by transfection experiments with COS-7 cells using the pEF.BOS-CD36 expression vector (Figure 6). The calculated kinetic constants were in accordance with our observation that CD36 protein expression was very low in COS-7 cells, whereas the cells transfected with pEF.BOS-CD36 vector expressed higher levels of CD36. Note that the arachidonate uptake was not normalized to the transfection efficiency of 20−30%.

CD36 is a 78−88-kDa cell surface glycoprotein present on monocyte/macrophages, platelets, adipose tissue, and microvascular endothelial cells. One of the striking features of CD36 is the wide and overlapping ligand-binding specificity. CD36 binds a variety of ligands, including thrombospondin (*57*), collagen (*58*), *Plasmodium falciparum*-infected erythrocytes (*59*, *60*), oxidized low-density lipoprotein (ox-LDL) (*61*), anionic phospholipids, apoptotic cells, and fatty acids (*22*, *62*). The functional significance of many of these receptor−ligand interactions is unknown. Studies with isolated and cultured cells have provided evidence that FAT/CD36 functions as a putative transporter of long-chain fatty acids. The participation of FAT/CD36 in FA uptake and metabolism in vivo has recently been shown by Coburn et al. (*63*). They presented data that the FA transport is reduced in heart, skeletal muscle, and adipose tissues of CD36 knockout mice.

Endothelial cells actively regulate their environment by secreting humoral substances, including endothelin-1 and a variety of eicosanoids, that have local actions. Under inflammatory conditions, endothelial cells respond to potential harmful conditions with the appropriate, adaptive changes in function and mediator release. A considerable body of evidence supports altered eicosanoid synthesis in profile and quantity upon cell activation. Endothelial cell-derived eicosanoids have been shown to regulate smooth muscle contractility and thrombocyte aggregation, and to modulate the adhesion of monocytes and neutrophils to endothelium. The hallmark of S100A8/A9 complexes is their accumulation at inflammatory loci as a consequence of specific secretion from activated leukocytes (*25*, *29*). These S100A8/A9 complexes have been shown to carry arachidonic acid (*24*) and are recognized by FAT/CD36 on endothelial cells as shown in the present study. Furthermore, endothelial cells utilize both endogenous and exogenous AA for transcellular production of eicosanoids (*7*). Together with the identification of FAT/CD36 as the major FA transporter on HUVEC, we speculate that the secreted S100A8/A9−AA complex may serve as a transport protein to move AA to its target cells. AA is then taken up by bystander cells to be metabolized to eicosanoids representing a particular transcellular pathway for AA metabolism. This mechanism may point to an important role in the initiation and regulation of the inflammatory response.

ACKNOWLEDGMENT

We thank Dr. Rick Thorne for kindly providing the pEF.BOS-CD36 expression vector, PD Dr. Beate Kehrel for helpful suggestions to CD36 purification, Dr. Annette Mehling for critical reading of the manuscript, and Silke Ladeur, Heike Hater, and Dieter Wiesmann for excellent technical assistance.

REFERENCES

1. Smith, W. L. (1989) *Biochem. J. 259*, 315−324.
2. Hajjar, D. P., and Pomerantz, K. B. (1992) *FASEB J. 6*, 2933−2941.
3. Goetzl, E. J., An, S., and Smith, W. L. (1995) *FASEB J. 9*, 1051−1058.
4. Cines, D. B., Pollak, E. S., Buck, C. A., Loscalzo, J., Zimmerman, G. A., McEver, R. P., Pober, J. S., Wick, T. M., Konkle, B. A., Schwartz, B. S., Barnathan, E. S., McCrae, K. R., Hug, B. A., Schmidt, A. M., and Stern, D. M. (1998) *Blood 91*, 3527−3261.
5. Serhan, C. N., Haeggstrom, J. Z., and Leslie, C. C. (1996) *FASEB J. 10*, 1147−1158.
6. Gerritsen, M. E. (1996) *Cardiovasc. Res. 32*, 720−732.
7. Karim, S., Habib, A., Levy-Toledano, S., and Maclouf, J. (1996) *J. Biol. Chem. 271*, 12042−12048.
8. Sala, A., Zarini, S., Folco, G., Murphy, R. C., and Henson, P. M. (1999) *J. Biol. Chem. 274*, 28264−28269.

9. Vyska, K., Meyer, W., Stremmel, W., Notohamiprodjo, G., Minami, K., Machulla, H. J., Gleichmann, U., Meyer, H., and Korfer, R. (1991) *Circ. Res. 69*, 857−870.
10. Krischer, S. M., Eisenmann, M., and Mueller, M. J. (1998) *Biochemistry 37*, 12884−12891.
11. Abumrad, N. A., Perkins, R. C., Park, J. H., and Park, C. R. (1981) *J. Biol. Chem. 256*, 9183−9191.
12. Stremmel, W. (1988) *J. Clin. Invest. 81*, 844−852.
13. Trigatti, B. L., Mangroo, D., and Gerber, G. E. (1991) *J. Biol. Chem. 266*, 22621−22625.
14. Abumrad, N. A., Park, J. H., and Park, C. R. (1984) *J. Biol. Chem. 259*, 8945−8953.
15. Mahadevan, S., and Sauer, F. (1974) *Arch. Biochem. Biophys. 164*, 185−193.
16. Harmon, C. M., Luce, P., Beth, A. H., and Abumrad, N. A. (1991) *J. Membr. Biol. 121*, 261−268.
17. Stremmel, W., Strohmeyer, G., and Berk, P. D. (1986) *Proc. Natl. Acad. Sci. U.S.A. 83*, 3584−3588.
18. Zhou, S. L., Stump, D., Sorrentino, D., Potter, B. J., and Berk, P. D. (1992) *J. Biol. Chem. 267*, 14456−14461.
19. Fujii, S., Kawaguchi, H., and Yasuda, H. (1987) *Arch. Biochem. Biophys. 254*, 552−558.
20. Schaffer, J. E., and Lodish, H. F. (1994) *Cell 79*, 427−436.
21. Harmon, C. M., and Abumrad, N. A. (1993) *J. Membr. Biol. 133*, 43−49.
22. Abumrad, N. A., El-Maghrabi, M. R., Amri, E. Z., Lopez, E., and Grimaldi, P. A. (1993) *J. Biol. Chem. 268*, 17665−17668.
23. Abumrad, N. A., Coburn, C., and Ibrahimi, A. (1999) *Biochim. Biophys. Acta 1441*, 4−13.
24. Kerkhoff, C., Klempt, M., Kaever, V., and Sorg, C. (1999) *J. Biol. Chem. 274*, 32672−32679.
25. Hetland, G., Talgo, G. J., and Fagerhol, M. K. (1998) *Mol. Pathol. 51*, 143−148.
26. Goebeler, M., Roth, J., Burwinkel, F., Vollmer, E., Bocker, W., and Sorg, C. (1994) *Transplantation 58*, 355−361.
27. Roth, J., Teigelkamp, S., Wilke, M., Grun, L., Tummler, B., and Sorg, C. (1992) *Immunobiology 186*, 304−314.
28. Brun, J. G., Jonsson, R., and Haga, H. J. (1994) *J. Rheumatol. 21*, 733−738.
29. Rammes, A., Roth, J., Goebeler, M., Klempt, M., Hartmann, M., and Sorg, C. (1997) *J. Biol. Chem. 272*, 9496−9502.
30. Kligman, D., and Hilt, D. C. (1988) *Trends Biochem. Sci. 13*, 437−443.
31. Kerkhoff, C., Klempt, M., and Sorg, C. (1998) *Biochim. Biophys. Acta 1448*, 200−211.
32. Zwadlo, G., Bruggen, J., Gerhards, G., Schlegel, R., and Sorg, C. (1988) *Clin. Exp. Immunol. 72*, 510−515.
33. Lagasse, E., and Clerc, R. G. (1988) *Mol. Cell. Biol. 8*, 2402−2410.
34. Klempt, M., Melkonyan, H., Nacken, W., Wiesmann, D., Holtkemper, U., and Sorg, C. (1997) *FEBS Lett. 408*, 81−84.
35. Siegenthaler, G., Roulin, K., Chatellard-Gruaz, D., Hotz, R., Saurat, J. H., Hellman, U., and Hagens, G. (1997) *J. Biol. Chem. 272*, 9371−9377.
36. Markwell, M. A. K. (1982) *Anal. Biochem. 125*, 427−432.
37. Oquendo, P., Hundt, E., Lawler, J., and Seed, B. (1989) *Cell 58*, 95−101.
38. Wyler, B., Daviet, L., Bortkiewicz, H., Bordet, J. C., and McGregor, J. L. (1993) *Thromb. Haemostasis 70*, 500−505.
39. Isola, L. M., Zhou, S. L., Kiang, C. L., Stump, D. D., Bradbury, M. W., and Berk, P. D. (1995) *Proc. Natl. Acad. Sci. U.S.A. 92*, 9866−9870.
40. Fitscher, B. A., Riedel, H. D., Young, K. C., and Stremmel, W. (1998) *Biochim. Biophys. Acta 1443*, 381−385.
41. Thorne, R. F., Meldrum, C. J., Harris, S. J., Dorahy, D. J., Shafren, D. R., Berndt, M. C., Burns, G. F., and Gibson, P. G. (1997) *Biochem. Biophys. Res. Commun. 240*, 812−818.
42. Melkonyan, H., Sorg, C., and Klempt, M. (1996) *Nucleic Acids Res. 24*, 4356−4357.
43. Kerkhoff, C., Vogl, T., Nacken, W., Sopalla, C., and Sorg, C. (1999) *FEBS Lett. 460*, 134−138.
44. Kronenberg, A., Grahl, H., and Kehrel, B. (1998) *Thromb. Haemostasis 79*, 1021−1024.
45. Laemmli, U. K. (1970) *Nature 227*, 680−685.
46. Smith, P. K., Krohn, R. I., Hermanson, G. T., Mallia, A. K., Gartner, F. H., Provenzano, M. D., Fujimoto, E. K., Goeke, N. M., Olson, B. J., and Klenk, D. C. (1985) *Anal. Biochem. 150*, 76−85.
47. Richieri, G. V., Anel, A., and Kleinfeld, A. M. (1993) *Biochemistry 32*, 7574−7580.
48. Subtil, A., and Dautry-Varsat, A. (1997) *J. Cell Sci. 110*, 2441−2447.
49. Durrbach, A., Louvard, D., and Coudrier, E. (1996) *J. Cell Sci. 109*, 457−465.
50. Kurashima, K., D'Souza, S., Szászi, K., Ramjeesingh, R., Orlowski, J., and Grinstein, S. (1999) *J. Biol. Chem. 274*, 29843−29849.
51. Kosower, N. S., and Kosower, E. M. (1987) *Methods Enzymol. 143*, 76−84.
52. Lefevre, P. G. (1975) *Curr. Top. Membr. Transp. 7*, 109−215.
53. Harmon, C. M., Luce, P., and Abumrad, N. A. (1992) *Biochem. Soc. Trans. 20*, 811−813.
54. Luiken, J. J., Turcotte, L. P., and Bonen, A. (1999) *J. Lipid Res. 40*, 1007−1016.
55. Berk, P. D., Wada, H., Horio, Y., Potter, B. J., Sorrentino, D., Zhou, S. L., Isola, L. M., Stump, D., Kiang, C. L., and Thung, S. (1990) *Proc. Natl. Acad. Sci. U.S.A. 87*, 3484−3488.
56. Stremmel, W. (1987) *J. Biol. Chem. 262*, 6284−6289.
57. Asch, A. S., Barnwell, J., Silverstein, R. L., and Nachman, R. L. (1987) *J. Clin. Invest. 79*, 1054−1061.
58. Tandon, N. N., Kralisz, U., and Jamieson, G. A. (1989) *J. Biol. Chem. 264*, 7576−7583.
59. Berendt, A. R., Simmons, D. L., Tansey, J., Newbold, C. I., and Marsh, K. (1989) *Nature 341*, 57−59.
60. McCormick, C. J., Craig, A., Roberts, D., Newbold, C. I., and Berendt, A. R. (1997) *J. Clin. Invest. 100*, 2521−2529.
61. Endemann, G., Stanton, L. W., Madden, K. S., Bryant, C. M., White, R. T., and Protter, A. A. (1993) *J. Biol. Chem. 268*, 11811−11816.
62. Febbraio, M., Abumrad, N. A., Hajjar, D. P., Sharma, K., Cheng, W., Pearce, S. F., and Silverstein, R. L. (1999) *J. Biol. Chem. 274*, 19055−19062.
63. Coburn, C. T., Knapp, F. F. Jr., Febbraio, M., Beets, A. L., Silverstein, R. L., Abumrad, N. A. (2000) *J. Biol. Chem. 275*, 32523−32529.

BI001791K